Cutaneous melanocytic tumors with concomitant NRAS Q61R and IDH1 R132C mutations: a report of six cases

Nicolas Macagno, Daniel Pissaloux, Heather Etchevers, Véronique Haddad, Béatrice Vergier, Sandrine Sierra-Fortuny, Franck Tirode, Arnaud de La Fouchardière

Running title: *NRAS* and *IDH1* co-mutated melanocytomas

Cutaneous melanocytic tumors with concomitant *NRAS*^{Q61R} and *IDH1*^{R132C} mutations: a report of six cases

Nicolas Macagno[1,4], Daniel Pissaloux[2,3], Heather Etchevers[4], Véronique Haddad[2], Béatrice Vergier[5], Sandrine Sierra-Fortuny[6], Franck Tirode[2,3], Arnaud de la Fouchardière[2,3]

1- *Department of Pathology, APHM, Timone, Marseille, France*
2- *Department of Biopathology, Centre Léon Bérard, Lyon, France*
3- *Université de Lyon, Université Claude Bernard Lyon 1, INSERM 1052, CNRS 5286, Centre Léon Bérard, Cancer Research Center of Lyon, Equipe Labellisée Ligue contre le Cancer, Lyon, France.*
4- *Aix Marseille Univ, INSERM, MMG, Marseille, France*
5- *Pathology Department, University Hospital of Bordeaux, Hôpital Haut-Lévêque, Bordeaux, France.*
6- *Cabinet de dermatologie, Le Mans, France*

Abstract

We report a series of six melanocytic proliferations harboring both *NRAS* and *IDH1* hotspot mutations.

Clinically, there was no specific sex-ratio, ages ranged from 18 to 85 years, and the trunk and limbs were the most affected localizations. In half of the cases, progressive modification of a pre-existing nevus was reported.

Morphologically, all tumors were predominantly based in the dermis and the most striking pathological finding was the presence of a background architecture of congenital-type nevi with a superimposed biphasic pattern formed by dendritic pigmented melanocytes surrounding areas of nevoid melanocytes. This finding was further underscored by HMB45 staining, which was positive in the dendritic cells and negative in the nevoid melanocytes. Four cases displayed increased cellularity and one case showed increased dermal mitotic activity. DNA and RNA sequencing revealed *NRAS*^{Q61R} *and IDH1*^{R132C} co-mutations in all six cases, with homogeneous expression data according to unsupervised clustering analysis. Array-CGH revealed no copy number alteration for the two most cellular and mitogenic cases. All were surgically excised, available follow-up for two patients showed no relapse nor metastases.

We hypothesize that the *IDH1* mutation is a secondary event in a pre-existing *NRAS*-mutated nevus and could be in part responsible for the emergence of a pigmented dendritic dermal component. So far, such co-mutations have been reported in one benign melanocytic nevus and several melanomas. This combination could represent a new subgroup of intermediate prognosis (melanocytoma) with a distinctive morphology. Further acquisition of genomic anomalies could progressively lead to malignant transformation.

ORCID:
Nicolas Macagno : 0000-0002-9882-2162
Daniel Pissaloux : 0000-0003-1118-950X
Heather Etchevers : 0000-0003-0201-3799
Béatrice Vergier : 0000-0002-3498-3143
Franck Tirode : 0000-0003-4731-7817
Arnaud De La Fouchardière: 0000-0003-2251-8241

Corresponding author:
Dr Nicolas Macagno MD, PhD
Department of Pathology
CHU Timone, AP-HM
13385, Marseille, France
Fax : + 33491384411
Phone : +33491380000
E-mail : nicolas.macagno@ap-hm.fr

Keywords: IDH1; R132C; Melanocytoma; Biphasic; Combined; NRAS; Nevoid; Dendritic; Spindle

Introduction

The recent WHO classification of skin tumors has expanded the group of intermediate grade lesions that occur during the progressive transition from a nevus to a melanoma. These proliferations are named low and high grade melanocytomas. The most frequent form of nevus in which such progression occurs is the common melanocytic nevus. They usually harbor either a *BRAF* or a *NRAS* hotspot mutation. These pigmented lesions are either congenital or acquired after birth, often after exposure to UV radiation. In this setting of a common nevus, several subgroups of clonal, intermediate neoplasms, have been identified and include combined deep penetrating nevi (DPN), *BAP1*-inactivated nevi (BIN) and combined Pigmented Epithelioid Melanocytomas (PEM). These subtypes are morphologically recognizable and have been respectively associated with the acquisition of *CTNNB1* (or *APC*) mutations, *BAP1*-inactivation or *PRKAR1A* bi-allelic loss within the clone. The acquisition of further genetic alterations can lead to malignant transformation in a small subset of these tumors. We report herein 6 melanocytic proliferations with both $NRAS^{Q61R}$ and $IDH1^{R132C}$ mutations that could represent a new subgroup of intermediate tumours (*i.e.* melanocytomas) with distinct morphological features.

Patients

All six cases in which both an activating point mutation in *NRAS* and *IDH1* were detected by sequencing techniques were received in consultation and reviewed at the Department of Biopathology at the Centre Léon Bérard in Lyon, France. Archived slides with hematoxylin, eosin, and phloxin (HPS) staining and immunohistochemistry (IHC) were reexamined for notable morphological and IHC details. Clinical information, including follow-up, was obtained from the referring pathologist or the clinician with signed consent of the patient for publication of clinical photographs. The study was conducted according to the Declaration of Helsinki and has been approved by the research ethics committee of the Centre Léon Bérard (ref: L20-08).

HMB45 immunohistochemistry

Sections from the paraffin blocks from each case were also stained for HMB45 (monoclonal, predilute, Biogenex) using the Ventana Benchmark Ultra automated immunostainer (Ventana Medical Systems (VMS), Tucson AZ) and revealed with the UltraView Universal DAB or RED Detection kit (Ventana).

Array CGH

Array-CGH was carried out for the two most cellular and mitogenic cases. DNA extraction was performed by macro-dissecting formalin-fixed paraffin-embedded tissue block sections followed by the use of the QIAamp DNA micro kit (Qiagen#56304, Hilden, DE). Fragmentation and labeling were done according to manufacturer's protocol (Agilent Technologies), using 1.5 µg of genomic DNA. Tumor DNA was labeled with Cy5, and a reference DNA (Promega#G1521or #G1471, Madison, USA) was labeled with Cy3. Labeled

samples were then purified using KREApure columns (Agilent Technologies #5190-0418). Labeling efficiency was calculated using a Nanodrop 2000 spectrophotometer. Co-hybridization was performed on 4x180K Agilent Sureprint G3 Human oligonucleotide arrays custom (Agilent Technologies #G4125A). Slides were washed, dried and scanned on the Agilent SureScan microarray scanner. Scanned images were processed using Agilent Feature Extraction software V11.5 and the analysis was carried out using the Agilent Genomic Workbench software V7.0.

RNA Sequencing

RNA sequencing was performed for all cases. Total RNA was extracted from macrodissected formalin-fixed paraffin-embedded tumor sections using the FormaPure RNA kit (Beckman Coulter #C19158, Brea, CA, USA). RNase-free DNase set (Qiagen #AM2222, Courtaboeuf, France) was used to remove DNA. RNA quantification was assessed using NanoDrop 2000 (ThermoFisher Scientific, Waltham, MA, USA) measurement and RNA quality using the DV200 value (the proportion of the RNA fragments larger than 200 nt) assessed by a TapeStation with Hs RNA ScreenTape (Agilent, Santa Clara, CA, USA). Samples with sufficient RNA quantity (>0.5 µg) and quality (DV200 > 30%) were further analyzed by RNA sequencing. One hundred nanograms of total RNA was used to prepare TruSeq RNA Exome libraries (Illumina #20020183, San Diego, USA). Twelve libraries were pooled at a concentration of 4 nM each, together with 1% PhiX. Sequencing was performed (paired end, 2 × 75 cycles) using NextSeq 500/550 High Output V2 kit on a NextSeq 500 machine (Illumina).

The mean number of reads per sample was around 80 million. Alignments were performed using STAR on the GRCh38 version of the human reference genome. Number of duplicate reads were assessed using PICARD tools. No sample was discarded from the analysis (number of unique reads above 10 million). Fusion transcripts were called by five different algorithms, including STAR-Fusion, FusionMap, FusionCatcher, TopHat-Fusion, and EricScript. Small Nucleotide Variation and InDels analyses were performed using GATK HaplotypeCaller (v3.5-0) and Annovar (2018-04-16 version). Expression values were extracted using Kallisto version 0.42.5 tool17 with GENECODE release 23-genome annotation based on the GRCh38 genome reference. Kallisto TPM expression values were transformed to log2(TPM+2), and all samples were normalized together using the quantile method from the R limma package within R (version 3.1.1) environment. Unsupervised clustering analysis was performed using Multi Experiment Viewer (MeV version 4.8.1).

DNA Sequencing

Multiplex library preparation was performed for one case using the STS_v1 Kit (Sophia Genetics, Saint Sulpice, Switzerland) according to the manufacturer's specifications with up to 50 ng of sample DNA. Hybridization capture of pooled libraries was performed using STS_v1 Kit (Sophia Genetics), including *BRAF* exons 11 and 15, *NRAS* exons 2 to 4, *HRAS* exons 2 to 4, *KIT* exons 8 to 11, exon 13, 17 and 18, *GNAQ* exons 4 and 5, *GNA11* exons 4 and 5, *TP53* full gene, *CDK4* exon 2, *CDKN2A* exons 1 to 3, *CTNNB1* exon 3, *MAP2K1* exons 2 and 3, and *hTERT* promoter region, from a global panel of 49 cancer genes. Captured libraries were sequenced as paired-end 150 bp reads on a MiniSeq instrument (Illumina). Sequence reads were

mapped to the reference human genome (hg19). Recalibration of reads, coverage, variant calling, and sequencing statistics were determined using the Sophia DDM platform.

Results

Clinical features

The clinical features of the patients harboring the tumors are listed in **Table 1**. The male to female sex ratio was 3M:3F and ages at diagnosis ranged from 18 to 85 y/o (median, 44 y/o). Sites of involvement were limbs, trunk and ear. Maximum diameters ranged from 4 to 11 mm (median, 6 mm). A history of progressive modification of a nevus known since childhood prompted the surgical excisional removal of three of the lesions (Cases n°3, 5 and 6). Clinical impression included suspicion of melanoma for two cases (case n°2 and n°4). The photography of case n°3 is provided (**Figure 1A**). Follow-up data was available for two patients and no local recurrence or metastatic spreading was observed.

Pathologic features

The histopathologic features of the six cases are summarized in **Table 2** and shown in **Figures 1-4**. The initial proposed diagnoses by referring pathologists encompassed atypical spitzoid tumor, MELTUMP, Deep Penetrating Nevus, and melanoma.

All cases appeared as predominantly dermal tumors, with a Breslow thickness ranging from 1.3 to 7.2 mm (mean, 3.5 mm). Slight and discontinuous lentiginous junctional activity was present in four cases and two cases were purely dermal. Low magnification silhouette (**Figure 1B,C,D,E,F,G**) encompassed a band-like growth for cases n°1 and n°2, exophytic dome-shaped growth for case n°3 and a more endophytic dermal growth, with a silhouette displaying a vertical deep expansion, for the remaining three cases.

The most striking feature was the presence of a biphasic pattern, consisting of fascicles of spindled dendritic melanocytes surrounding areas of bland nevoid melanocytes (**Figure 2A, B**), with formation of well-delineated nevoid islands in four cases (**Figure 2**). Nevoid cells were densely packed, with scant cytoplasm and an oval, bland nucleus with inconspicuous nucleolus. The spindled component was arranged in short storiform or haphazard fascicles and displayed more abundant eosinophilic cytoplasm, a vesicular nucleus with open chromatin and a basophilic nucleolus. Pigmentation was low and melanophages were scarce or absent. Peripheral cells were disposed in an interstitial pattern, with entrapment of collagen bundles reminiscent of dermatofibroma in two cases (**Figure 2**). Stroma was either absent, slightly myxoid, loose edematous, and/or elastotic. An inflammatory lymphoid infiltrate was present in 2 cases.

In more than half of the cases, histological findings suggestive of a congenital-type nevus were present, distorted however by the dermal growth: focal or continuous band of epithelioid pigmented nests in the superficial dermis in 4 cases (66%), grenz zone in 5 cases (83%), splaying and single filing of melanocytes in long rows between collagen bundles in 5 cases (83%) and an adnexal or perivascular intrication in 4 cases (66%).

Considering atypical features, mild nuclear atypia was present in three cases, without high-grade pleomorphism. Four cases displayed higher cell density with dermal overgrowth. All cases lacked a clear vertical maturation. None displayed ulceration, pagetoid scatter, necrosis, angioinvasion or neurotropism.

Case n°3, clinically associated with a recent modification, displayed involvement of the papillary dermis, a slight asymmetry, higher cell density, mild atypia, nuclear overlap, and an increased dermal mitotic activity (2 mitoses/mm^2), without high-grade cytologic atypia or all criteria for nevoid melanoma. In this specific case, Ki67 stained 5-10% of nuclei and no clonal loss of p16 expression nor p53 nuclear overexpression was observed.

Immunohistochemical results

HMB45 highlighted the biphasic architecture with positivity of the scattered dendritic melanocytes, whereas nevoid melanocytes were negative in all cases. HMB45-positive dendritic melanocytes were randomly scattered within the tumor, with variable density at the periphery or within the deepest portion of the neoplasm. Junctional lentiginous activity was highlighted by HMB45 in four cases, and dermal top-heavy HMB45 staining was lacking in 2 cases. **(Figure 3A)**

Molecular results

All cases found by RNA-sequencing analysis showed a mutation in *IDH1* resulting in p.Arg132Cys (R132C), co-occurring with a mutation in *NRAS*, resulting in p.Gln61Arg (Q61R). One case was confirmed by DNA sequencing for both mutations. Unsupervised hierarchical clustering analysis based on transcriptomic data revealed that all *IDH1* melanocytomas were grouped together in a robust cluster, separated from a control group of 10 *NRAS*-mutated melanomas and 3 giant congenital *NRAS*-mutated nevi (**Figure 3G**). The two cases with the densest dermal component were studied by array-comparative genomic hybridization to rule out the diagnosis of melanoma. They displayed normal cytogenetic profiles, without any chromosomal imbalances or segmental gains or losses.

Discussion

Genetic mutations modifying function of enzymes related to cellular metabolism have been reported in various malignancies. Four main enzymes can be affected: isocitrate dehydrogenase 1 (IDH1) and 2 (IDH2), succinate dehydrogenase (SDH) and fumarate hydratase (FH).

Mutations of *IDH1/2* have been reported in gliomas and secondary glioblastoma, cartilaginous tumors and chondrosarcoma, acute myeloid leukemia, and cholangiocarcinoma. Pathological mutations induce a single substitution of a specific arginine residue within their catalytic sites, affecting Arg132 in IDH1 and Arg172 or Arg140 in IDH2, respectively.[1] These recurrent mutations lead to the abnormal accumulation of D-2-hydroxyglutarate, which is an oncometabolite[2] that consequently induces epigenetic modifications and transcription of

oncogenic pathways. Mutations of *IDH1* and *IDH2* are nearly always mutually exclusive; reports of co-occurrence are exceptional.[3] Non-canonical variants have also been reported at a low-frequency in thyroid, esophageal, colorectal, prostate and breast carcinomas, with unknown or uncertain significance with respect to pathogenesis.

In melanocytic proliferations, mutations of *IDH1* affecting the Arg132 residue have also been reported, but always in combination with hotspot *NRAS* mutations. This is an important distinction, as these *NRAS* mutations are already present in congenital nevi, in which they are considered as a MAP-kinase pathway activating driver alteration. In this setting, the *IDH1* mutation should be considered as a secondary event.

The TCGA genomic classification of melanomas emphasizes that a distinct CpG island methylator phenotype (CIMP) defines a specific subgroup of melanoma.[4] This subgroup is enriched for *NRAS* and *IDH1* mutations, notably $IDH1^{R132C}$. In a previous study, the CIMP was associated with melanoma progression.[5] A CIMP has also been reported to be triggered by *IDH* mutations in various malignancies, notably gliomas.[6] Linos *et al.* have recently identified the combination of concomitant *NRAS* and *IDH1* mutations in 6/214 patients with advanced stage or metastatic melanoma,[7] but its putative role in the progression of melanoma is currently unknown and still debated.[8,9] So far, only a single case of a common melanocytic nevus with both anomalies has been reported, but without any morphological detail.[10]

We report herein the clinical, morphological and genetic data of six cases of difficult-to-classify melanocytic proliferations, with co-existing *NRAS* and *IDH1* mutations and for which a diagnosis of melanoma was excluded. Clinically, these lesions had been removed in adults because of recent modification of a previously known pigmented lesion, but no specific site was noted. No clinical relapse was observed.

Morphological analysis was informative, because none of these cases appeared to be a standard compound nevus. This observation differs from the classic description of combined nevi, in which a background common nevus is frequently identified in the periphery of a clonal proliferation such as in *BAP1*-inactivated nevi or combined deep penetrating nevi.[11,12] Instead, in our cases, only some architectural features of an underlying congenital-type nevus were seen (such as a band-like distribution in the superficial dermis with small nests of type-A pigmented melanocytes) but distorted, with a superimposed biphasic morphology. This dermal pattern showed pigmented dendritic melanocytes surrounding areas of nevoid melanocytes. This nested nevoid component was reminiscent of the dermal component commonly observed in NRAS-mutated congenital nevi.

The HMB45 staining pattern further underscored the biphasic pattern, with positivity in the dendritic cells and negativity in the nevoid melanocytes. We hypothesize that similarly to what is observed in nevi with *BAP1* or *CTNNB1* mutations, $IDH1^{R132}$ mutations may induce this specific histological pattern in a *NRAS* mutated nevus. In this intermediate stage, some variable degrees of atypia were observed, which led to the request for a consultant's opinion. These atypia included increased dermal cell density, mild cyto-nuclear pleomorphism or limited mitotic activity. The degree of pigmentation was rather low in all cases, including the scarcity of melanophages. All our cases were either classified as low- or high-grade melanocytomas. In two cases, array-CGH was performed to exclude a diagnosis of melanoma. Both showed a readout devoid of anomalies.

It is difficult to be certain how these lesions might have been labelled in the past, but the features we describe match the description of combined blue nevus. In a study of 511 combined nevi, combined blue nevus represented 66% of the cases including 11% with atypical features.[13] Unfortunately, there was no genetic data in that study. With regards to the apparent rarity of the lesions we describe, it is plausible that other molecular alterations, yet to be described, could be found in this morphological group with a similar biphasic pattern.

In contrast, no specific pattern was noted in morphological features of the six melanomas with both *NRAS* and *IDH1* mutations reported by Linos *et al*.[7] Likewise, we reviewed the available digital whole-slide images for six of the TCGA melanoma samples with *NRAS* Q61 and *IDH1* R132 mutations and found no relevant morphological patterns. The diversity of the acquired oncogenic events leading to malignant transformation could hypothetically explain these results.

Our unsupervised clustering data of melanocytic proliferations mutated in exon 3 of *NRAS* supports several hypotheses, having segregated the three benign common nevi from the group of six "melanocytomas". The ten melanomas clustered in several smaller groups, in agreement with their higher morphological heterogeneity, but again in distinct clusters. The unique case of melanoma presenting the canonical co-mutations of *NRAS* and *IDH1* clustered with other melanomas rather than with our six cases presenting the same mutations. These results bring an independent validation to the distinction of each subgroup but also support an additional level of complexity introduced by the combination of genetic alterations that are present in melanomas. This has been amply supported by Shain et al., including in *NRAS* or *BRAF*-mutated melanomas *ex nevus*.[14]

Several cases of melanomas with co-occurrence of *BRAF* and *IDH1* mutations have also been reported, but their benign or intermediate counterparts have yet to be described and they may harbor a completely different morphology.[7,15] $IDH1^{R132}$ mutations conferred a growth advantage to $BRAF^{V600E}$-mutated melanoma cells *in vitro* and in xenografts, but not to *BRAF*-wildtype melanoma cells.[15]

On prognosis grounds, *IDH1* mutations carry a strong and independent prognostic value for gliomas, but it has not been reported for acute myeloid leukemia or chondrosarcoma. In melanomas, TCGA data revealed no link to overall survival (log-rank, $p = 0.603$) or progression free survival (log-rank, $p = 0.945$).

Conclusion

We report a series of six unclassified melanocytic proliferations with a co-occurrence of $NRAS^{Q61R}$ *and* $IDH1^{R132C}$. They displayed homogeneous morphological features: in a background of a congenital-like nevus silhouette, a dermal biphasic pattern associated bland nevoid and scattered dendritic melanocytes with some degree of cytological and architectural atypia. No evidence of malignancy was observed. This description fills in the gap between the previously reported nevi and melanomas harboring both of these mutations, which could form a new group of melanocytomas in this genetic and clinical setting. These lesions morphologically resemble the description of previously reported "combined blue nevus", suggesting that further genetic studies should be performed in this latter group.

Authors' contributions

AF conceived the study and provided the cases. NM and AF collected and analyzed the clinical and histopathological data, and wrote, edited, and reviewed the manuscript. DP, FT, VH, performed the molecular analysis of the samples. BV contributed one case and reviewed the manuscript. HE reviewed the manuscript. SSF and BV contributed one case and reviewed the manuscript.

Compliance with ethical standards

The study was conducted according to the Declaration of Helsinki and has been approved by the research ethics committee of the Centre Léon Bérard, Lyon, France (Ref: L20-08).

Acknowledgments

The authors thank all referring pathologists that have provided case materials: Maxime Vernez, Caroline Lacoste, Guillaume Granier, Marie-Laure Petit, Catherine Feutry – and dermatologists: Sandrine Buscaylet-Colling, Franck Delesalle, Olivier Pegorier, Florence Hoareau, Emeline Kubica. We thank Rossita Lavoza for sharing her feedback on the nevus case she reported. Part of the data utilized in this study were generated by the TCGA Research Network: https://www.cancer.gov/tcga.

References

1. Yang H, Ye D, Guan K-L, et al. IDH1 and IDH2 mutations in tumorigenesis: mechanistic insights and clinical perspectives. *Clin. Cancer Res. Off. J. Am. Assoc. Cancer Res.* 2012;18:5562. doi:10.1158/1078-0432.CCR-12-1773.

2. Xu W, Yang H, Liu Y, et al. Oncometabolite 2-Hydroxyglutarate Is a Competitive Inhibitor of α-Ketoglutarate-Dependent Dioxygenases. *Cancer Cell* 2011;19:17–30. doi:10.1016/j.ccr.2010.12.014.

3. Hartmann C, Meyer J, Balss J, et al. Type and frequency of IDH1 and IDH2 mutations are related to astrocytic and oligodendroglial differentiation and age: a study of 1,010 diffuse gliomas. *Acta Neuropathol. (Berl.)* 2009;118:469–474. doi:10.1007/s00401-009-0561-9.

4. Cancer Genome Atlas Network. Genomic Classification of Cutaneous Melanoma. *Cell* 2015;161:1681–1696. doi:10.1016/j.cell.2015.05.044.

5. Tanemura A, Terando AM, Sim M-S, et al. CpG Island Methylator Phenotype Predicts Progression of Malignant Melanoma. *Clin. Cancer Res.* 2009;15:1801–1807. doi:10.1158/1078-0432.CCR-08-1361.

6. Malta TM, de Souza CF, Sabedot TS, et al. Glioma CpG island methylator phenotype (G-CIMP): biological and clinical implications. *Neuro-Oncol.* 2018;20:608–620. doi:10.1093/neuonc/nox183.

7. Linos K, Tafe LJ. Isocitrate dehydrogenase 1 mutations in melanoma frequently co-occur with NRAS mutations. *Histopathology* 2018;73:963–968. doi:10.1111/his.13707.

8. Hodis E, Watson IR, Kryukov GV, et al. A Landscape of Driver Mutations in Melanoma. *Cell* 2012;150:251–263. doi:10.1016/j.cell.2012.06.024.

9. Hodis E, Garraway LA. Molecular Genetics of Melanocytic Neoplasia. In: Fisher DE, Bastian BC, eds. *Melanoma*. New York, NY: Springer New York; 2017:1–23. doi:10.1007/978-1-4614-7322-0_29-1.

10. Lazova R, Pornputtapong N, Halaban R, et al. Spitz nevi and Spitzoid melanomas: exome sequencing and comparison with conventional melanocytic nevi and melanomas. *Mod. Pathol. Off. J. U. S. Can. Acad. Pathol. Inc* 2017;30:640–649. doi:10.1038/modpathol.2016.237.

11. Wiesner T, Murali R, Fried I, et al. A Distinct Subset of Atypical Spitz Tumors is Characterized by BRAF Mutation and Loss of BAP1 Expression: *Am. J. Surg. Pathol.* 2012;36:818–830. doi:10.1097/PAS.0b013e3182498be5.

12. Yeh I, Lang UE, Durieux E, et al. Combined activation of MAP kinase pathway and β-catenin signaling cause deep penetrating nevi. *Nat. Commun.* 2017;8:644. doi:10.1038/s41467-017-00758-3.

13. Baran JL, Duncan LM. Combined Melanocytic Nevi: Histologic Variants and Melanoma Mimics. *Am. J. Surg. Pathol.* 2011;35:1540–1548. doi:10.1097/PAS.0b013e31822e9f5e.

14. Shain AH, Yeh I, Kovalyshyn I, et al. The Genetic Evolution of Melanoma from Precursor Lesions. *N. Engl. J. Med.* 2015;373:1926–1936. doi:10.1056/NEJMoa1502583.

15. Shibata T, Kokubu A, Miyamoto M, et al. Mutant IDH1 confers an in vivo growth in a melanoma cell line with BRAF mutation. *Am. J. Pathol.* 2011;178:1395–1402. doi:10.1016/j.ajpath.2010.12.011.

Table 1 : Main clinical features of the six IDH1-NRAS biphasic melanocytomas

Case No.	Age (Years)	Sex	Localization	Pre-existing nevus	Diameter (mm)	Follow-up
1	85	M	Trunk	Unknown	4	N/A
2	27	F	Trunk	Unknown	11	N/A
3	66	M	Lower limb	Present	8	NOD (2 years)
4	18	F	Upper limb	*de novo*	6	N/A
5	23	M	Upper limb	Present	6	N/A
6	47	F	Ear	Present	7	NOD (6 months)

N/A : Not Available; NOD : No evidence of Disease

Table 2 : main histological features of the six IDH1-RAS biphasic melanocytomas

Case No.	Silhouette	Depth (mm)	Mitotic activity (1 mm^2)	Nuclear atypia	Biphasic pattern	HMB45	Congenital-type nevus features
1	Band-like	3,2	0	Mild	Islands	Scattered dendritic	BOE, GZ, SSFM, API
2	Band-like	2,2	0	Mild	Islands	Scattered dendritic	GZ, SSFM, API
3	Exophytic dome	1,3	2	Mild	Mixed	Scattered dendritic	BOE, SSFM, API
4	Vertical deep expansion	2,2	0	none	Mixed	Scattered dendritic	BOE, GZ, SSFM, API
5	Vertical deep expansion	4,8	1	none	Islands	Scattered dendritic	GZ, SSFM
6	Vertical deep expansion	7,2	0	none	Islands	Scattered dendritic	BOE, GZ

BOE : band of epithelioid pigmented nests, GZ : grenz zone, SSFM : splaying or single-filing of melanocytes, API : Adnexal or Perivascular intrication

Figure legends

Figure 1. Overview of melanocytic neoplasms with co-mutation of *IDH1* and *NRAS*.
A. Clinical photograph (case n°3).
B-C. Superficial horizontal band-like silhouette (cases n°1 and 2).
D. Exophytic, dome-shaped silhouette, with the papillary dermis involvement (case n°3).
E-F-G. Endophytic dermal growth silhouette (cases n°4, 5 & 6).

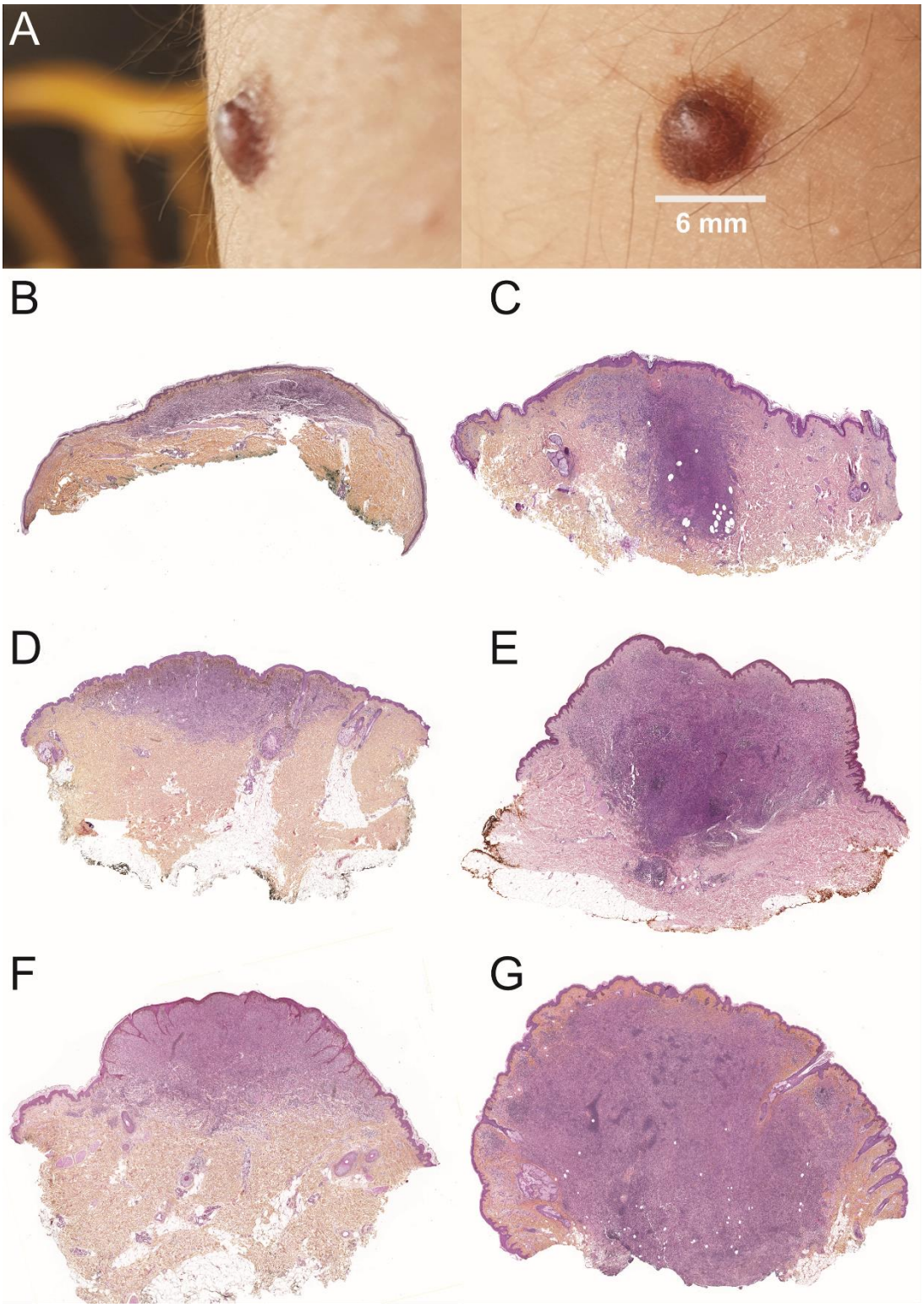

Figure 2. Histological characteristics

A. Dermal band-like biphasic nevoid/spindle proliferation without junctional activity and nests of epithelioid pigmented melanocytes in superficial dermis (case n°1).
B. At the periphery, a dermatofibroma-like interstitial pattern, with entrapment of collagen bundle by the spindled component. Congenital-type pattern with intricated melanocytes within the arrector pilores muscle. A nevoid island is present (arrowhead) (case n°2).
C. A band of pigmented epithelioid nests at the top, with scattered melanophages and a dense dermal biphasic proliferation. (case n°3).
D. Biphasic dermal pattern, with storiform arrangement of the spindle component, islands of nevoid melanocytes and a slight inflammatory response (case n°4).
E. Atypical case with higher cellularity, involvement of papillary dermis, a slight reticular epiderma hyperplasia, without ulceration. The biphasic pattern is more visible at the bottom and periphery. (case n°5).
F. A dense dermal tumor with a bright biphasic pattern, forming well-defined islands of nevoid melanocytes engulfed within an abundant and dense spindled component. Grenz zone is spared and epithelioid pigmented nests are present at the top. (case n°6).

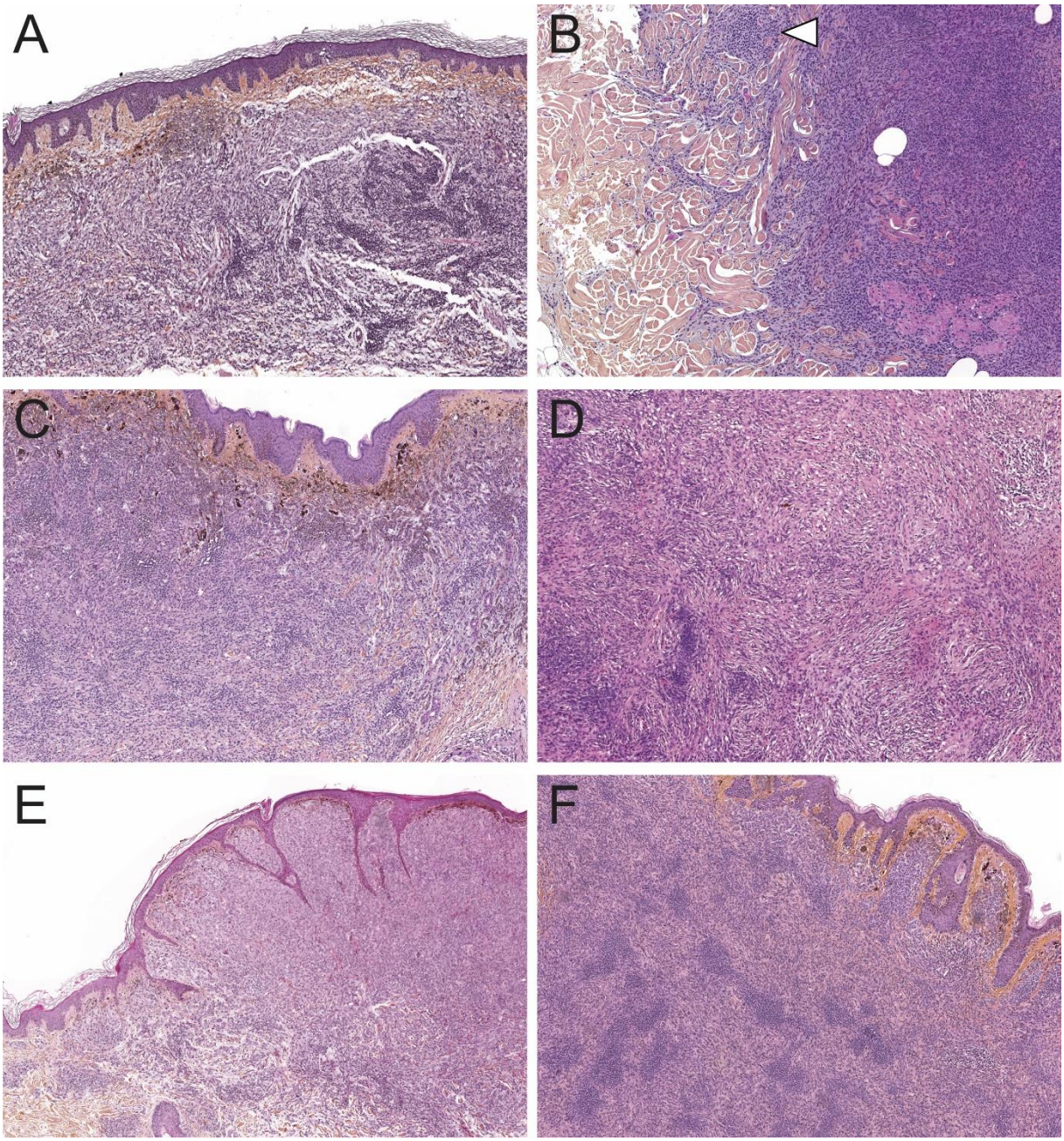
A
B
C
D
E
F

Figure 3. Histological characteristics (continued), immunostains and hierarchical clustering.

A. Higher magnification of the biphasic pattern: nevoid islands surrounded by short haphazard fascicles of spindled dendritic melanocytes (Case n°6).
B. HMB45 stains numerous scattered dermal dendritic melanocytes within the spindled component but does not stain nevoid islands.
C. Higher cellularity, mild nuclear atypia and mitotic activity (arrowhead) in this atypical case (Case n°3).
D. Higher magnification of scattered dermal melanocytes highlighted by HMB45.
E. Unsupervised clustering based on transcriptomic data: separation of all *IDH1* melanocytomas in a robust cluster, separated from a control group of 10 *NRAS*-mutated melanomas and 3 giant congenital *NRAS*-mutated nevi